frontiers in Marine Science

ORIGINAL RESEARCH
published: 19 June 2020
doi: 10.3389/fmars.2020.00465

Iridocytes Mediate Photonic Cooperation Between Giant Clams (Tridacninae) and Their Photosynthetic Symbionts

Susann Rossbach[1]†, Ram Chandra Subedi[2]†, Tien Khee Ng[2], Boon S. Ooi[2] and Carlos M. Duarte[1]*

[1] Red Sea Research Centre and Computational Bioscience Research Center, Biological and Environmental Science and Engineering Division, King Abdullah University of Science and Technology, Thuwal, Saudi Arabia, [2] Photonics Laboratory, Computer, Electrical and Mathematical Sciences and Engineering Division, King Abdullah University of Science and Technology, Thuwal, Saudi Arabia

OPEN ACCESS

Edited by:
Carla Zilberberg, Federal University of Rio de Janeiro, Brazil

Reviewed by:
Miguel Mies, University of São Paulo, Brazil
Anthony William Larkum, University of Technology Sydney, Australia

***Correspondence:**
Susann Rossbach
susann.rossbach@kaust.edu.sa; susannrossbach@hotmail.com

†*These authors have contributed equally to this work*

Specialty section:
This article was submitted to Coral Reef Research, a section of the journal Frontiers in Marine Science

Received: *30 January 2020*
Accepted: *25 May 2020*
Published: *19 June 2020*

Citation:
Rossbach S, Subedi RC, Ng TK, Ooi BS and Duarte CM (2020) Iridocytes Mediate Photonic Cooperation Between Giant Clams (Tridacninae) and Their Photosynthetic Symbionts. Front. Mar. Sci. 7:465. doi: 10.3389/fmars.2020.00465

Iridocytes, containing multiple stacks of proteinaceous platelets and crystalized guanine, alternating with thin cytoplasm sheets, are specialized cells that act as multilayer nano-reflectors. Convergence evolution led to their arising across a broad range of organisms, including giant clams of the Tridacninae subfamily – the only sessile and photosymbiotic organism, among animals known to possess iridocytes. Through the interference of light with their nanoscale architecture, iridocytes generate "structural colors," which are reported to serve different purposes, from intra-species communication to camouflage. In giant clams, iridocytes were previously reported to promote a lateral- and forward scattering of photosynthetically productive radiation (PAR) into the clam tissue, as well as the back reflection of non-productive wavelengths. Hence, they are assumed to promote an increased efficiency in the use of available solar energy, while simultaneously preventing photodamage of the algal symbionts. We report the use of guanine crystals within *Tridacna maxima* giant clam iridocytes as a basis for photonic cooperation between the bivalve host and their photosynthetic symbionts. Our results suggest that, in addition to the previously described scattering processes, iridocytes absorb potentially damaging UV radiation (UVR) and, through successive emission, emit light at longer wavelengths, which is then absorbed by the photosynthetic pigments of the algal symbionts. Consequently, both, host and algal symbionts are sheltered from (potentially) damaging UVR, while the available solar energy within the PAR spectrum increases, thereby potentially enhancing photosynthetic and calcification rates in this large bivalve. Further, our results suggest that this photonic cooperation could be responsible for the broad repertoire of colors that characterizes the highly diverse mantle patterns found in *T. maxima*.

Keywords: *Tridacna*, photosynthesis, iridocyte, symbiosis, light, giant clam

INTRODUCTION

Iridocytes (also called iridophores, guanophores, or interference cells) are multilayer nano-reflectors with alternating high and low refractive indices, generating interference of light waves. They contain multiple stacks of thin proteinaceous platelets (Kamishima, 1990; Griffiths et al., 1992; Kim et al., 2017) and crystalized guanine (Morrison et al., 1996; Teyssier et al., 2015) (an essential component of DNA and RNA), alternating with thin sheets of cytoplasm (Ide and Hama, 1972; Rohrlich and Rubin, 1975; Kim et al., 2017). Convergence evolution has led to their arising across a broad range of organisms, including reptiles, such as chameleons (Rohrlich and Rubin, 1975), amphibians, such as tree frogs (Setoguti, 1967), fish (Lythgoe et al., 1984), and mollusks such as cephalopods (Cloney and Brocco, 1983; DeMartini et al., 2013a) and giant clams of the Tridacninae subfamily (Kamishima, 1990; Griffiths et al., 1992; Holt et al., 2014; Ghoshal et al., 2016a).

Iridocytes display a variety of different functions in organisms, from the prevention of gas diffusion (Scholander, 1954), protection against extreme heat (Kobelt and Linsenmair, 1992), as mirror components of visual systems (Locket, 1970) and the manipulation of light (Fox, 1976; Holt et al., 2014; Ghoshal et al., 2016a; Kim et al., 2017). Through the interference of light with a combination of their nanoscale architectures, iridocytes generate some of the liveliest colorations across these organisms (Holt et al., 2014; Teyssier et al., 2015).The resulting "structural colors" (Fox, 1976) are reported to serve different purposes, from intra-species communication (Chae and Nishida, 1994) to camouflage (Théry and Casas, 2002; Ikeda and Kohshima, 2009).

Recent research mainly focused on "how nanostructures, such as Iridocytes, regulate the optical properties of biological materials" (Sun et al., 2013). However, photonic structures in biological systems were recently reported to also potentially affect physiological processes in plants and phototrophic organisms in general (Gkikas et al., 2015; Goessling et al., 2018). The structural nature of iridocytes allows them to reflect any waveband of the visible light spectrum from near UV to deep red (400–700 nm) (Mäthger and Hanlon, 2007). Further, there is evidence that organisms may be able to change the optical properties of these cells from non-iridescent (Rayleigh-scattering) to iridescent (structural reflection) by ultrastructural changes, thereby allowing rapidly shifts in skin colors (Mäthger and Hanlon, 2007; DeMartini et al., 2013a,b).

Giant clams of the Tridacninae subfamily stand out among all other organisms containing iridocytes as the sole sessile organisms thus far reported to contain these specialized cells. In Tridacninae, iridocytes are located in the outer mantle of the bivalve (Griffiths et al., 1992; Holt et al., 2014; Ghoshal et al., 2016a) which confer these animals their distinct and highly diverse mantle colors (Holt et al., 2014; Ghoshal et al., 2016a; **Figure 1**). Giant clams represent an important component of Indo-Pacific reef communities and are of distinct ecological significance for a reef (Neo and Todd, 2013; Neo et al., 2015; Van Wynsberge et al., 2016).They play multiple roles in the framework of coral reef communities (Neo et al., 2015), as they provide a food source for a number of predators and scavengers (Alcazar, 1986), shelter for commensal organisms (De Grave, 1999), and

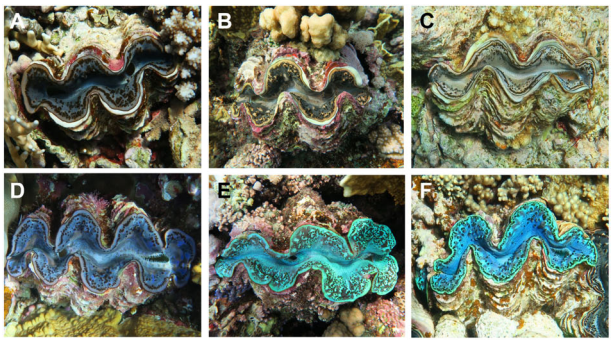

FIGURE 1 | Variations of mantle tissue colorations in Tridacninae, here exemplarily shown for *Tridacna maxima*. Specimens in the top row **(A–C)** are examples for brown color variants and those in the bottom **(D–F)** for blue appearing mantle colorations. Panels **(C,F)**, respectively, are equivalents for the brown and blue variation used in this study.

substrate for epibionts (Vicentuan-Cabaitan et al., 2014), and also have been harvested by humans for food and ornamental purposes (Mies et al., 2017). Further, they are even considered an ecosystem-engineering species (Neo et al., 2015) as they may form reef-like structures (Andréfouët et al., 2005).

Giant clams are one of the few molluscan groups that live in symbiotic relationship with unicellular algae of the Symbiodiniaceae family (Taylor, 1969; Yonge, 1975; Norton et al., 1992; Fitt, 1993). Among all the animals that are currently known to possess iridocytes, this symbiosis makes them the only organism capable of photosynthesis, through the activity of their algal symbionts. These symbionts are located intercellularly in a special tubular system, originating in digestive diverticular ducts of the stomach and extending into the outer mantle (Norton et al., 1992). As the algal symbionts can deliver up to 100% of the respiratory carbon demand of giant clams (Trench et al., 1981; Klumpp et al., 1992; Klumpp and Griffiths, 1994), some species are even considered to be net (photo)-autotrophs (Klumpp and Griffiths, 1994; Jantzen et al., 2008). This successful photo-symbiotic relationship is considered to be the main reason why Tridacninae are among the largest (Beckvar, 1981) and fastest-growing (Bonham, 1965) bivalves on Earth, and why bleaching (i.e., the loss of their symbiotic algae) (Glynn, 1993; Norton et al., 1995) is known to significantly decrease their fitness, resulting in reduced growth, fecundity, and survival (Leggat et al., 2003; Maboloc et al., 2015). Besides their contribution to the gross physiological performance of giant clams, the photosymbiotic relationship of Tridacninae and Symbiodiniaceae is probably also one of the reasons why the calcification in these bivalves is strongly light-dependent (Ip et al., 2017, 2018; Chew et al., 2019; Rossbach et al., 2019).

Unlike the many other mollusks, amphibians, fishes, and reptiles containing iridocytes, in Tridacninae the role of these cells would be unrelated to interactions with conspecifics or potential predators or competitors (e.g., camouflage or intimidation). Thus, previous studies, examining optical properties and the functional significance of iridocytes in giant clams either suggest their function to be acting as some kind of sunscreen (Yonge, 1975; Ishikura et al., 1997) or to

enhance photosynthetic rates of the algal symbionts by forward-scattering of light (Holt et al., 2014; Ghoshal et al., 2016a). As the requirements of their symbionts for photosynthetically active radiation (PAR, 400–700 nm) restrict Tridacninae to sunlit and shallow waters, giant clams expose themselves and their algal symbionts to potentially high levels of environmental ultraviolet radiation (UVR, 280–400 nm) (Smith and Baker, 1979). These highly energetic wavelengths are known to cause photo-inhibition in the associated algae, therefore leading to detrimental effects on the photosynthetic performance (Lesser and Shick, 1989; Lesser, 2006). In giant clams, UV-B (280–320 nm) and UV-A (320–400 nm) have been previously shown to completely suppress photosynthesis in isolated Symbiodiniaceae, while having little effect on the symbionts when embedded within the clam host tissue (Ishikura et al., 1997). Photo-protective mechanisms in Tridacninae have been previously mainly attributed to the presence of UV-absorbing compounds (e.g., mycosporine-like amino acids, MAAs), which are produced by the algal symbionts and deposited in the giant clam mantle tissues (Banaszak et al., 2006; DeBoer et al., 2012). Recent research shows that the iridocyte cells, produced by the giant clams themselves, may also have an important function in the protection against (potentially) harmful wavelengths of light (Holt et al., 2014; Ghoshal et al., 2016a). On the basis of models and experimental assessment of the spectral light penetration into tissues, iridocytes in Tridacninae were previously reported to promote a lateral- and forward scattering of photosynthetically productive wavelengths of light into the clam host tissue, as well as the back reflection of non-productive wavelengths (Holt et al., 2014; Kim et al., 2017). By providing these unique features, they are assumed to establish optimal conditions for the photosynthetic performance of the giant clams' symbionts (Holt et al., 2014; Ghoshal et al., 2016a).

In the present study, we assess the photoluminescence (PL) of *Tridacna maxima* giant clam iridocytes (embedded in the clams' outer mantle tissues) as well as of pure guanine, the material which composes the optically active components of the iridocytes. Further, we characterize different properties of *T. maxima* mantle tissues using scanning electron microscopy (SEM) and transmission electron microscopy (TEM).

MATERIALS AND METHODS

Collection of Clams

In August 2018, two specimens (one brown and one blue color variant) of the giant clam *T. maxima,* both with a size of about 17 cm, were collected in a water depth of about 3 m at Abu Shosha reef in the Central Red Sea (22.303833 N, 39.048278 E).

Tissue Characterization Using Scanning Electron Microscopy and Transmission Electron Microscopy

Tissue sample preparation for SEM imaging followed a standard protocol. In brief, pieces of *T. maxima* outer mantle tissues of approximately 25 mm^2 area were fixed overnight in a 2–2.5% glutaraldehyde in 0.1 M cacodylate buffer at a temperature of 4°C. After that, tissues were gently washed in the 0.1 M cacodylate buffer. Post fixation was performed in the dark, using a 1% osmium tetroxide in the cacodylate buffer for 1 h. The clam tissues were then washed with deionized water three times, keeping them in the water for at least 15 min, before they were dehydrated using ethanol with increasing concentration (30, 50, 70, 90, and 100%). Following this procedure, tissues were dried using critical point drying (CPD) for approximately 2 h. At last, they were coated with a 4 nm thin layer of platinum, to avoid charging effects while performing the SEM imaging. Imaging was conducted using a Quanta 3D FEG SEM (FEI, Netherlands).

For the blockphase SEM and TEM imaging, biopsy punches (approximately 1 mm^2) of the *T. maxima* mantle tissue were fixed and embedded in Durcupan ACM resin (EMS, United States), following the protocol by Deerinck et al. (2010). Block phase SEM imaging was performed using a Teneo VS^{TM} SEM (Thermo Fisher Scientific, United States). For the TEM imaging, the embedded mantle tissues were cut into 140 nm thin sections using a Leica Ultramicrotome EM UC7 (Leica, Germany) and images were taken with a Titan CT TEM (Thermo Fisher Scientific, United States).

Absorbance Spectra of *T. maxima* Mantle Tissues

For the absorbance measurements, outer mantle tissues were sliced into layers of 0.5 mm thickness and mounted onto double side polished sapphire substrates. The measurements were carried out on two sets of samples: (a) at the outermost surface of the tissue and (b) inside mantle tissues (about 500 μm deep from the surface), using a UV–Vis–NIR spectrophotometer (Shimadzu UV-3600).

Setup for Photoluminescence Measurements

The Labram Aramis set up (Horiba Scientific, Japan) was used to measure the PL of the giant clam mantle tissues (**Supplementary Figure 1**). This compact and automated system allows to easily choose the excitation source and power from the LabSpec6 software (Horiba Scientific, Japan). Three different laser excitation sources were used: Helium Cadmium (325 nm), Cobalt 06-MLD (473 nm), and Melles Griot (633 nm). Samples of *T. maxima* tissues were placed on a sapphire substrate and then positioned on the probing stage of the measurement setup. The laser was focused on the tissue sample with a 40-fold magnification objective, resulting in a spot size of approximately 5 μm. Minimizing the spot size was necessary in order to increase the power intensity of the laser, as a smaller spot size resulted in a smaller area and thus higher laser intensity, as:

$$\text{Power intensity} = \frac{\text{Power}}{\text{Area of laser spot}}$$

For every scan, the laser source was automatically cut-off right after a completed scan to minimize potential damages of the tissues due to continuous exposure. The planar and vertical adjustment of the stage, using LabSpec6, allows a fine resolution as low as 1 μm.

PL Measurements of Giant Clam Mantle Tissue

Mantle clippings of approximately 1 mm in thickness and a cross-section area of about 1 cm^2 of *T. maxima* were used for the subsequent measurements. When the clam mantle tissues were optically probed, multi-peak PL emissions were observed. First, PL measurements were performed on the mantle surface (where the laser source was focused at the surface i.e., $Z = 0$ μm). To understand how the light propagates deep inside the tissue, subsequent PL emission spectra were taken at different focal depth inside the mantle tissue as deep as ∼300 μm. Second, in order to explore how the *T. maxima* tissues interact with different light sources and excitation power, they were probed with different excitation sources of wavelengths at 325, 473, and 633 nm and various pumping. In order to understand the interaction of the light with *T. maxima* tissues and the resulting dependent PL spectra, several measurements with excitation sources of wavelengths at 325, 473, and 633 nm were conducted at room temperature. Further, we performed excitation power-dependent PL measurements (**Supplementary Figure 2**). The type of charge carrier recombination (free to bound and/or donor-acceptor pair recombination) contributing to the PL can be further explored by plotting integrated photoluminescence (IPL) versus the power of the excitation source. Further, the quantum yield was calculated using the following relation:

$$\text{Quantum Yield} = \frac{\text{Integrated photoluminescence intensity}}{\text{Integrated excitation source intensity}}$$

The quantum yield was averaged (with a 95% confidence interval) from measurements on five individual tissue samples.

PL Measurements of Pure Guanine Powder

Commercially available guanine powder (3,4-(Methylenedioxy) cinnamic acid) with a 99% assay (Sigma Aldrich, United States), was desiccated at room temperature. An approximately 1 mm thick layer of crystalline guanine powder was put on the sapphire substrate and the prepared sample was subjected to the PL test in the Labram Aramis spectrometer setup (Horiba Scientific, Japan) following the same procedure as for the giant clam mantle tissue.

RESULTS

Mantle Tissue Characteristics of *T. maxima*

Observations of the *T. maxima* outer mantle tissues, using SEM, revealed surface structures with hexagonal features (**Figure 2A**), consisting of pillar-like microstructures (**Figures 2B,C**), where each of these pillars has an average length of about 1 μm (**Figures 2C,D**). Below the surface layer, we find the embedded symbiotic unicellular algae (**Figure 3A**), stacked in pillars and located extracellularly in a tubular system.

In close proximity, the iridocyte cells can be found (**Figure 3B**). They have of similar dimensions as the neighboring Symbiodiniaceae (e.g., diameter of 8 μm) and TEM imaging reveals the plate-like structure of proteinaceous material and crystalized guanine within the iridocyte cells, alternating with thin cytoplasm sheets (**Figures 3C,D**).

Absorbance of *T. maxima* Mantle Tissues

Absorbance spectra of *T. maxima* mantle tissues differed with depth into the tissue (i.e., outermost surface tissue and at 500 μm inside the mantle tissue) (**Figure 4**). We observed strong absorbances throughout the UV spectra (200–400 nm) at both depths. Whereas the absorbance in the outermost mantle tissues decreases with wavelengths >330 nm, absorbance spectra of tissue layers deeper inside the mantle, at about 500 μm, shows a strong imprint of photosynthetic pigments, with a broad shoulder between 400 and 560 nm, a relative absorbance minima around 600 nm, and another, distinct peak in absorbance around 675 nm, corresponding to chlorophyll *a*.

Conversion of UV-A Wavelengths Into the Blue Part of the Spectrum

When mantle tissues of the giant clam *T. maxima* (**Figure 5A**) were illuminated with UV-A (325 nm) radiation, the PL emitted by the mantle tissues, located between the surface and 300 μm into the mantle of the animal, shifted toward longer wavelengths, resulting in a broadened emission peak, ranging from 550 to 365 nm (**Figure 5B**, see schematic of the general absorption/emission mechanism in **Supplementary Figures 4, 5**). Multiple peaks were observed in the PL spectra when the tissue was probed at each of the different focal depths. However, the most intense peak was identified as the main peak (**Figures 5B,C**).

Indeed, the dominant emission peaks under UV-A (325 nm) excitation, shift from 365 nm at 300 μm depth into the tissue, to 550 nm at the surface of the giant clam mantle. Closer inspection of the spectral emission shifts with depth showed a gradual increase of peak shift rates from the mantle surface ($Z = 0$ μm) to about 100 μm (0.803 nm μm^{-1} at 100 μm) tissue depth, and a decrease in peak shift rates deeper into the tissue (**Figures 5C–E**). The calculated quantum yield was 39.20 ± 4.16 (mean ± SD) (**Supplementary Figure 6**).

Comparison Between Emission Spectra of Iridocytes and Pure Guanine

Exciting the *T. maxima* mantle tissues with a laser source within the red part of the spectrum (633 nm) resulted in a peak emission at 673 nm with a shoulder at 733 nm (**Figure 6A** and **Supplementary Table 1**). Excitation with wavelengths within the blue spectra (473 nm) resulted in an intense peak at 673 nm with a shoulder at 734 nm (**Figure 6A**). Under UV-A (325 nm) excitation, three emission maxima are apparent in the spectra, (1) a strong peak in the violet spectrum at 391 nm, (2) a broad shoulder in the green around 530 nm, and (3) and a smaller peak at 676 nm (**Figure 6A**).

While investigating PL spectra of pure guanine, by exciting them with identical laser excitation sources (633, 473, and 325 nm, respectively), no emission signal (other than noise) was detected when exciting pure guanine with red irradiance at a

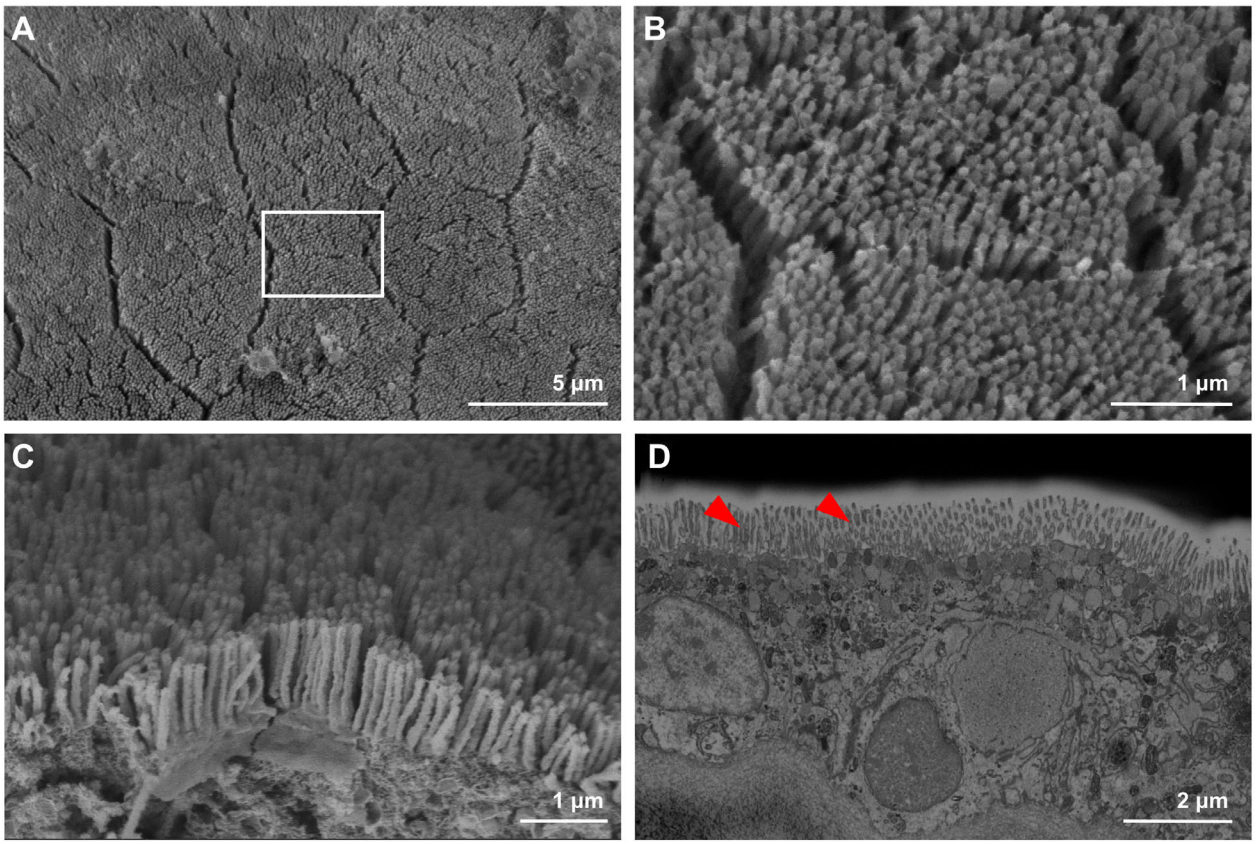

FIGURE 2 | Mantle surface structures of *T. maxima*, observed via and scanning electroscope microscopy (SEM). **(A)** Overview of mantle surface, with hexagonal features. **(B,C)** Magnified top view of mantle surface, revealing pillar-like microstructures. **(D)** Blockphase SEM of cross-sectioned mantle tissue showing topmost 10 µm, including pillar-like microstructures, highlighted by red arrows.

wavelength of 633 nm (**Figure 6B** and **Supplementary Table 2**). However, emission spectra peaked at 500 nm when excited with a 473 nm source and at 363 nm with a shoulder at 414 nm when excited with 325 nm (**Figure 6B**).

When then compared the PL spectra of the *T. maxima* mantle tissues with those of the pure guanine crystals. In guanine, the peak in the upper UV-A spectrum (around 360–390 nm) was conserved, although it was broad and somewhat shifted to longer, less energetic wavelengths than in the *T. maxima* tissues (391 nm maxima in giant clam tissues versus 363 nm in pure guanine). While *T. maxima* showed a clear emission peak at 676 nm when excited with a light source of 473nm generated an emission peak at 676 nm, the emission peak at 530 nm in the pure guanine was barely visible in the emission spectra.

DISCUSSION

Surface Structures of Outer *T. maxima* Mantle

The observed microstructures on the outer layer of the *T. maxima* outer mantle tissues could be potentially part of a light-harvesting system, just as some comparable photonic nanostructures on butterfly wings (Vértesy et al., 2006; Tam et al., 2013) and bird feathers (Eliason et al., 2015) have been previously reported being responsible for controlling how incident light is reflected and scattered. For the butterflies, differences in iridescence were also reported to be due to a difference in those nanostructures, including their optical thickness and the periodicities of air/cuticle bilayer stacks (Tam et al., 2013). Should the observed micro-pillar structures on the surface of the giant clam mantle tissues serve a comparable function it is therefore possible, that both, their length as well as the density of these micropillars could influence the amount, and thus the intensity of light that penetrates the mantle surface, reaching deeper tissue layers.

Absorbance Spectra and Conversion of UV Radiation Into Blue Light

The mantle tissues of *T. maxima* showed strong absorbance in the UVR band (200–400 nm) for both probed tissue depths (i.e., outermost surface and at a deeper layer of about 500 µm tissue depth) (**Figure 4**). While absorbance at the photosynthetically active range (PAR, 400–700 nm) were only minor in the outermost tissues, the innermost tissues (at about 500 µm tissue depth) showed the absorbance spectra characteristic of

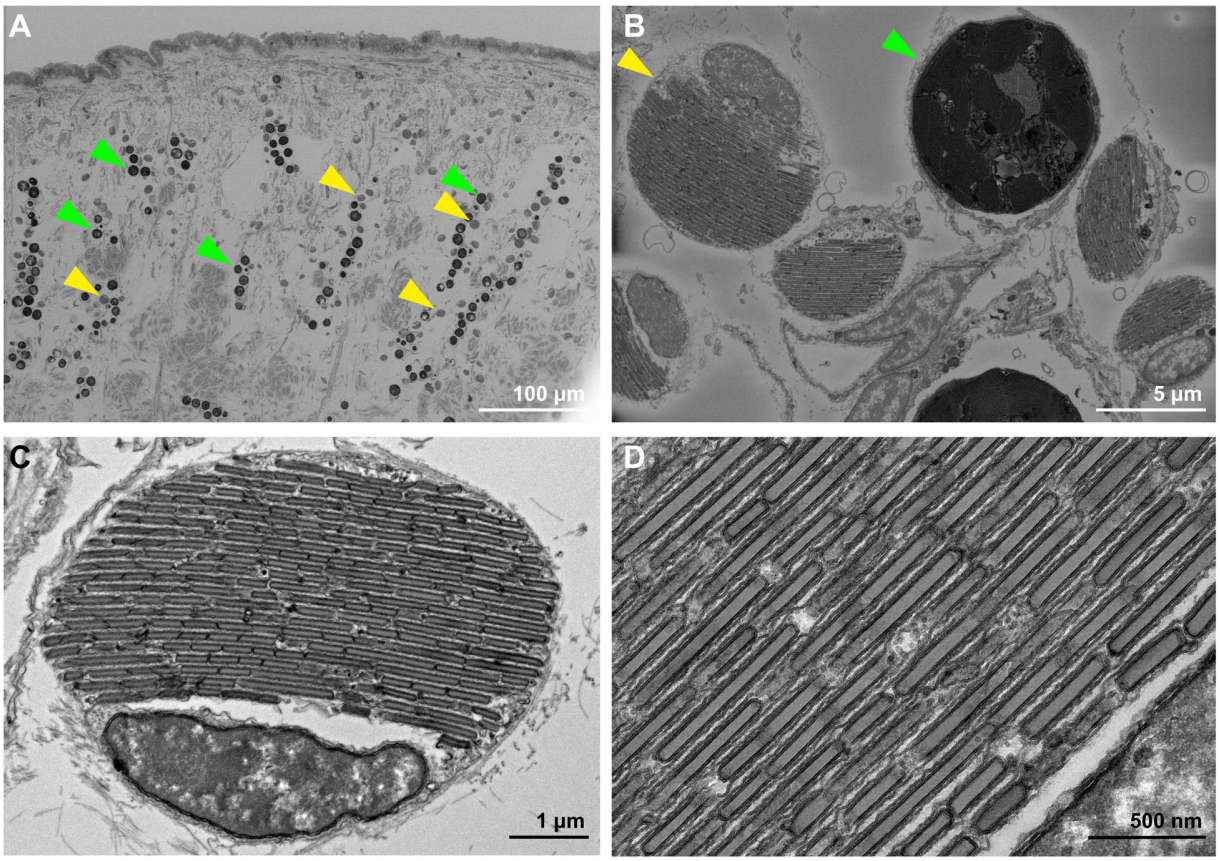

FIGURE 3 | (A) Blockphase SEM image of cross-sectioned *T. maxima* mantle tissues, from the surface to about 400 µm deep into the tissue. Symbiotic algae are stacked in pillars and highlighted with green arrows, iridocytes can be found in close proximity and are highlighted with yellow arrows. **(B)** Magnified view of algal symbionts (green arrow) and iridocytes (yellow arrow). Both have an average diameter of about 8 µm. **(C)** TEM image of iridocyte cell with stacked layers of crystalized guanine plates, alternating with cytoplasm sheets. **(D)** TEM image of magnified view on Iridocyte cell, showing crystalized guanine plates.

photosynthetic pigments in the PAR range. Here, light is harvested by the photosynthetic antenna system of the algal symbionts, resulting in the broad shoulder between 400 and 560 nm, an absorbance minima around 600 nm, and a peak in absorbance around 675 nm. The remarkable difference in absorbance spectra between outermost layer, with a strong imprint from iridocytes, and the deeper tissues is probably due to a lack of symbionts within the surface tissues of the mantle. As already shown by Holt et al. (2014), iridocytes cells are organized in the tissue in a diffuse layer within the outermost tissues (first 100–200 µm) and on top of the algae pillars, which can be mainly found deeper within the tissue.

A number of previous studies have already investigated giant clam iridocyte cells and their three-dimensional system of brightly reflective structures on the basis of models and experimental assessment of the spectral light penetration into tissues (e.g., Holt et al., 2014; Ghoshal et al., 2016a,b; Kim et al., 2017). These specialized cells have been proposed to promote a lateral- and forward scattering of photosynthetically productive wavelengths of light into the clam host tissue, as well as the back reflection of non-productive wavelengths (Holt et al., 2014; Ghoshal et al., 2016a; Kim et al., 2017). This "redistribution" is assumed to promote an increased efficiency in the use of available solar energy, while simultaneously preventing photodamage of the algal symbionts (Holt et al., 2014; Ghoshal et al., 2016a).

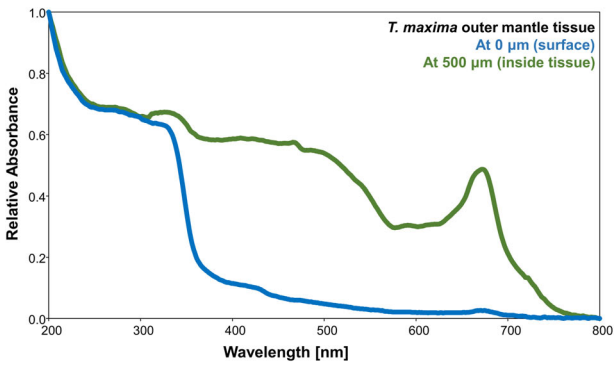

FIGURE 4 | Relative absorbance of wavelengths between 200 and 800 nm of *T. maxima* outer mantle tissues for two different tissue depths: outermost surface tissues (blue) and inside the tissues, at a depth of about 500 µm from the surface (green).

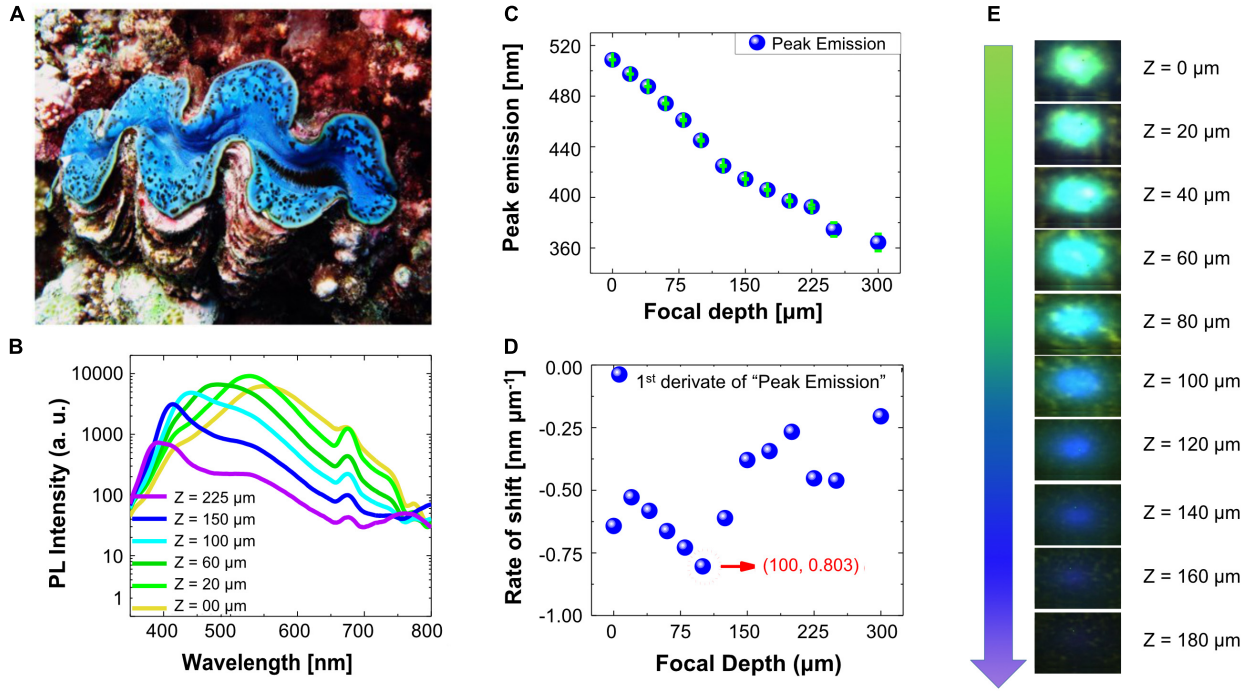

FIGURE 5 | (A) Photo of *T. maxima* specimen with blue mantle coloration. **(B)** Photoluminescence (PL) spectra of T. maxima at room temperature for different focal depths (exemplarily shown for six focal depths, ranging from mantle surface to 225 µm within the tissue). **(C)** Peak emission wavelengths (nm) of *T. maxima* photoluminescence versus focal depth (µm). Green bars represent the standard error, obtained by a Gaussian fit. **(D)** Rate of peak shift (nm μm^{-1}) in *T. maxima* photoluminescence versus focal depth (µm). **(E)** Illustration showing the color changes in PL with varying focal depth (*Z*), where $Z = 0$ is directly at the giant clam mantle surface and $Z > 0$ indicates measurements deeper inside the mantle tissue.

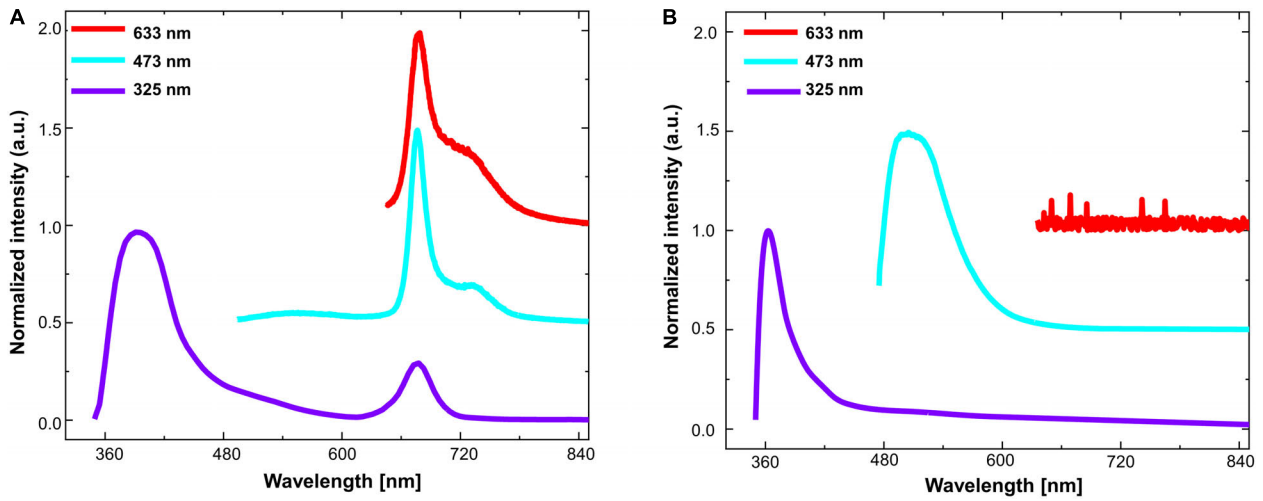

FIGURE 6 | Photoluminescence spectra (at room temperature) under three different laser excitation sources: at 633 nm (red), 473 nm (blue), and 325 nm (violet), respectively for **(A)** *Tridacna maxima* mantle tissues and **(B)** pure guanine powder.

However, our observations further indicate that, in addition to the previously described backscattering of non-productive wavelengths, giant clam iridocytes are also able to absorb UVR and re-emit it, shifted toward longer wavelengths. This finding further contributes to mitigate potential impacts of UVR (Häder et al., 2007; Llabrés et al., 2013; Häder et al., 2015), while enhancing photosynthetically available radiation to the symbionts. Highly energetic UVR has been reported to have significant and often detrimental effects on processes and different life stages of marine organisms (Llabrés et al., 2013), such as DNA damage and oxidative stress (Shick et al., 1995; Shick et al., 1996; Van De Poll et al., 2001), decreased growth

and calcification (Van De Poll et al., 2001; Gao and Zheng, 2010), reduced photosynthesis (Lesser, 1996; Gao and Zheng, 2010; Regaudie-de-Gioux et al., 2014), and changes in respiration (Agustí et al., 2014), as well as adverse effects on reproduction, larval development and settlement (Aranda et al., 2011; Carreja et al., 2016) and increased mortality rates, especially during early life stages (Gleason and Wellington, 1995; Béland et al., 1999; Al-Aidaroos et al., 2014). As a result of the continuous environmental pressure from UVR, especially on shallow-water communities of tropical oceans, many organisms developed effective defense systems. To date, there are two processes described for marine organisms to protect themselves against harmful UVR: (1) use of reflective structures, as in the case of the planktonic algae and coccolithophorid *Emiliania huxleyi.* The coccolith structures, calcium carbonate plates on the outside of these algae, show a backscatter between 25 and 50% of the incoming UVR (Gordon and Du, 2001; Quintero-Torres et al., 2006) and (2) use of UV-absorbing compounds, as reported for a wide range of different organisms, from algae to arthropods, mollusks, fish, cnidarians, protozoans, and others (Sinha et al., 2007; Núñez-Pons et al., 2018). As for giant clams, a previous study on the potential UV-protective properties of *T. crocea* reported the presence of MAAs in the giant clams' mantle tissue (Ishikura et al., 1997). These compounds are known for their photo protective functions as they absorb wavelengths in the UV spectrum (Shick et al., 1992; Banaszak et al., 2006).

Our present results suggest that, in addition to the known processes of UV-absorption by MAAs and the potential backscattering of highly energetic wavelengths by the iridocytes, *Tridacna* iridocytes also absorb potentially harmful wavelengths within the UV spectrum and re-emit radiation shifted into photosynthetically active wavelengths (400–700nm) that can be used by their photosynthetic symbionts. Together, these simultaneous effects of photo-protection and efficient use of available solar energy help explain why Tridacninae are able to thrive in very shallow waters (1 m water depth or less), where UVR levels are very high – especially in tropical oceans (Overmans and Agustí, 2019, 2020).

Cooperation Between Iridocytes and Algal Symbionts

As the only photosymbiotic organism among iridocyte-containing animals, Tridacninae contain dinoflagellate algal symbionts (Symbiodiniaceae), and therefore also their photosynthetic antenna systems, including photosynthetic pigments, such as chlorophyll *a* and *c*. The contribution of chlorophyll *a* is clearly visible in the unique and well-known emission peak at around 676 nm (Holm-Hansen and Riemann, 1978), where it can absorb the blue light emitted by the guanine. Thereby harmful UVR is shifted into photosynthetically active blue radiation, which is in turn absorbed by the chlorophyll, and ultimately emitted as innocuous, "waste" far-red radiation. Blue light emitted by guanine that is not absorbed by chlorophyll may then be again absorbed by the guanine of the iridocytes. The iridocytes may then re-emit at a longer wavelength, yielding the broad emission shoulder in the green color (at about 530 nm) characterized here for pure, crystalized guanine, as well for the tissue-embedded iridocytes (**Figures 5B**, **6A**). Light at wavelengths around 530 nm can then be further absorbed by a unique photosynthetic antenna system (i.e., the peridinin–chlorophyll *a*–protein – PCP), which harvests light in the green region (530–550 nm) and is characteristic of dinoflagellates, including Symbiodiniaceae (Larkum, 1996; Kanazawa et al., 2014).

The photonic cooperation between the iridocytes cells of the giant clam host, and the photosynthetic chlorophyll pigments contained within the algal symbiont cells contributes to the protection of both, giant clam and symbiont, from harmful UVR while potentially also increasing the supply of PAR (400–700nm) to the symbionts. As the requirements of their algal symbionts for PAR (400–700nm) restricts Tridacninae to sunlit, shallow waters, giant clams have to expose themselves and their symbionts to potentially high levels of environmental UVR (280–400nm). This is especially true for the tropical waters (Smith and Baker, 1979) inhabited by Tridacninae, such as the very transparent waters of the Red Sea where the animals tested here grew. Particularly the highly energetic wavelengths within the UV spectrum are known to lead to photo-inhibition in the associated algae and to have therefore detrimental effects on their photosynthetic performance (Lesser and Shick, 1989; Lesser, 1996; Shick et al., 1996). In giant clams UVR has been previously shown to completely suppress photosynthesis in isolated zooxanthellae while having little effect on the symbionts when embedded within the giant clam host tissue (Ishikura et al., 1997). Until now, this photo-protective effect has been mainly attributed to the UV-absorbing properties of MAAs and it was proposed that the symbiotic algae are thus protected from UVR damage by their host tissues (Ishikura et al., 1997). Mycosporine-like amino acids are however, actually produced by the algal symbionts and then deposited in the giant clam mantle tissues. In fact, *Tridacna* spp. have been reported to associate with dinoflagellates of the genus *Symbiodinium*, *Cladocopium* and *Durusdinium* (Mies, 2019) (former clade A, C, and D; LaJeunesse et al., 2018). Red Sea giant clams have been reported to associate mostly with the *Symbiodinium* genus (Pappas et al., 2017) (former clade A), which are known for their ability to produce MAAs (Banaszak et al., 2000).

However, while MAAs and the associated UV-protection would be provided by the algal symbionts, iridocyte cells are actually produced by the bivalve host itself. This interaction between host-owned cells and the embedded algae would emphasize how the mutualistic component of the symbiotic relationship of Tridacninae and Symbiodiniaceae extends to protection from UVR. Further, this interaction is absent from photosymbiotic relationship of Symbiodiniaceae and corals, where the latter have to rely on the production of MAAs and the consequent photo-protection through their algal symbionts (Rosic and Dove, 2011). Moreover, this stresses again that, although the relationship of Symbiodiniaceae with corals and with giant clams, respectively, are comparable in many ways (e.g., the provision of shelter, carbon, nitrogen, and other inorganic nutrients by the host to their algal symbionts, and simultaneous supply of photosynthetic metabolites by

the symbiotic dinoflagellates to the host), some components, specifically the interactions driven by the iridocytes, of these symbioses are functionally different.

Models and assessments of the spectral light penetration into giant clam tissues, previously reported iridocytes in Tridacninae to promote a lateral- and forward scattering of photosynthetically productive wavelengths of light into the clam host tissue, as well as the back reflection of non-productive wavelengths (Holt et al., 2014). Hence, they presumably establish optimal conditions for the photosynthetic performance of the clams' symbionts (Holt et al., 2014; Ghoshal et al., 2016a).

Comparable mechanisms of light harvest through biological nano- and microstructures and a resulting increase in photosynthetic efficiency have been recently also reported for other organisms (Jacobs et al., 2016; Goessling et al., 2018, 2019). As in the case of the centric diatom *Coscinodiscus granii*, light redistribution and thus increased efficiency in photosynthesis in cell regions outside the directly illuminated area were affected by the optical properties of the frustule valves (Goessling et al., 2018, 2019). Likewise, in Begonia leaves, the brilliant blue iridescence, caused by specialized chloroplasts, is assumed to improve photosynthetic quantum efficiencies, especially under low light conditions (Jacobs et al., 2016). In giant clams, the process of converting harmful UVR into photosynthetically active and still highly energetic blue radiation may also contribute to support the high rates of carbonate deposition and shell growth that have been reported for Tridacninae (Bonham, 1965; Ip et al., 2018; Chew et al., 2019; Rossbach et al., 2019). Both, indirectly, as elevated photosynthetic rates will lead to high internal pH and a high saturation state for carbonate minerals, thereby favoring calcification (McConnaughey and Whelan, 1997) and directly, as blue light (i.e., highly energetic light) emitted by the iridocytes exposed to UVR, has been suggested to directly stimulate calcification rates (Cohen et al., 2016; Ip et al., 2017).

High absorption of UVR by guanine has been known for decades, however, mostly in the context of mutations in DNA due to the production of the oxidized form of guanine when exposed to UVR – the main reason why UVR is mutagenic (Kawanishi et al., 2001; Ravanat et al., 2001). However, the role of guanine crystals in iridocytes has received attention only recently. Holt et al. (2014) modeled, based on spectral shifts of irradiance with depth into the *Tridacna* tissue, the photo-protective role of giant clam role iridocytes. The present experimental data extends these efforts by providing evidence that, in addition to reflection, iridocytes in the *T. maxima* mantle tissues show a clear absorbance of UVR wavelengths (200–400 nm; **Figure 4**), consistent with the UVR absorption of pure guanine. Therefore, our results identify a dual role of iridocytes, protecting the animal from high-energetic wavelengths (including UVR), while enhancing the flux of PAR to the symbiont by shifting the UVR radiation absorbed into longer wavelengths within the PAR range, where they can be used by the photosynthetic symbionts. Further, our results provided evidence that the re-emitted longer wavelengths are in fact contributed by guanine (as shown in **Figure 6B**), the material which composes the optically active components of the iridocytes in Tridacninae, as well as similar guanine-containing structures in other animals (e.g., squid, octopus, and chameleon) (Rohrlich and Rubin, 1975; Cloney and Brocco, 1983; Teyssier et al., 2015).

Photonic Cooperation Leads to the Rich Color Palette and Patterns of Giant Clam Mantles

The photonic cooperation between guanine crystals within the iridocytes of giant clams and chlorophyll, contributed by the symbiotic algae, also generates the broad repertoire of colors that characterizes the distinct and highly diverse mantle colors found in giant clams, e.g., *T. maxima* (**Figure 1**). The variety of apparent colors may be derived from different intensities of violet (391 nm), green (530 nm), and red (676 nm) emission peaks. Indeed, our results suggest that where chlorophyll *a* levels are particularly high, relative to iridocyte levels, the mantle coloration would appear reddish-brown (i.e., dominance of

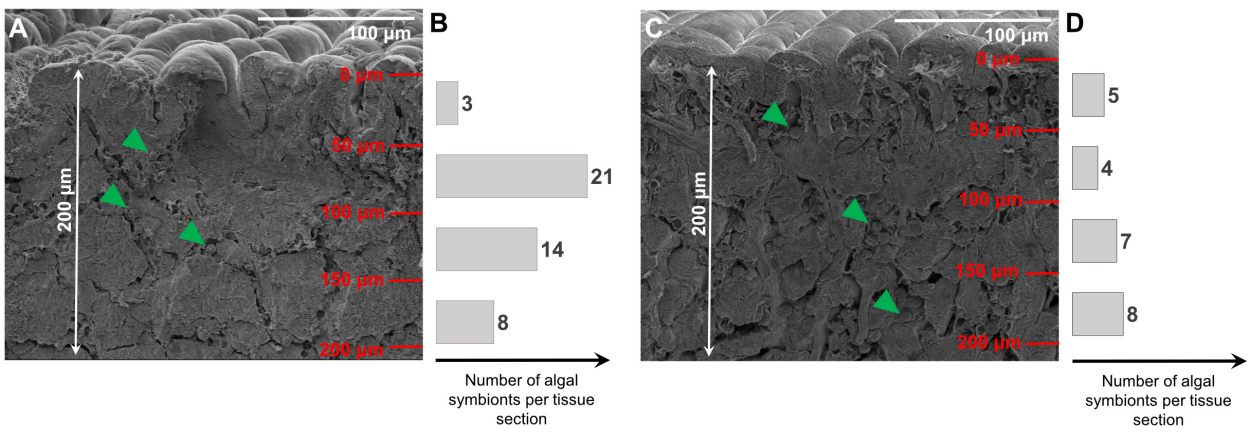

FIGURE 7 | SEM pictures of first 200 µm of mantle tissue in a brown **(A)** and blue **(C)** phenotype of *T. maxima*. Bar plots represent numbers of Symbiodiniaceae in tissue at four different tissue layers (50 µm increments), from tissue surface to a depth of 200 µm into the mantle tissue. Algal symbionts (Symbiodiniaceae) are exemplarily highlighted with green arrows. Numbers of algal symbionts within each tissue section are presented as bars for the brown **(B)** and blue phenotype **(D)**.

673 nm emission peak), whereas high iridocyte levels may lead to blue mantle coloration (i.e., dominance of 391 nm; **Figure 1**). Hence, by shifting the relative abundance of chlorophyll *a* relative to iridocytes, or their distribution within the mantle, an individual animal could shift mantle colors, ranging from blue to green and brown. A difference in relative abundances of Symbiodiniaceae and their distribution within the first 200μm of the *T. maxima* mantle of a brown (**Figure 7A**) and blue (**Figure 7C**) phenotype is exemplarily illustrated in **Figure 7**. Brown phenotypes would, therefore, overall harbor more algal symbionts as blue phenotypes. Further, the pattern of distribution of the algae within the tissue and between different tissue depths varies (as exemplarily shown in **Figures 7B,D**, respectively).

Therefore, our experimental data show that, unlike assumed in the past (Kamishima, 1990; Holt et al., 2014), giant clams of different apparent colors are not intrinsically different in optical properties. In addition, the observed nanostructures, found on the surface of the giant clam mantle tissues could have an influence on the light-harvesting and photonic proprieties, and thus apparent color variants in *T. maxima.* The range of coloration characteristic of *T. maxima* within individuals may also derive from spectral shifts in incoming light, as solar radiation penetrates into the ocean and is progressively depleted of the red wavelengths, being strongly absorbed by pure water and phytoplankton. Between Tridacninae species, however, the concentration of iridocyte cells differs (Holt et al., 2014), and *T. maxima* has been reported to display some of the highest variabilities in coloration, hence possibly also highest concentration of iridocytes. Further research would therefore be needed to confirm if the differences in colorations in other Tridacninae species would be likewise influenced by a "Mix-and Match" of algal symbionts and iridocytes.

CONCLUSION

Our findings confirm that giant clam iridocytes convert potentially damaging radiation into light emitted in the blue part of the spectrum, which can be subsequently absorbed by the photosynthetic pigments of the algal symbionts. This dual mechanism, where bivalve host and symbionts are sheltered from damaging UVR, while the flux of PAR increases, provides a major advantage to Tridacninae due to two reasons: (1) the exposure to high doses of UVR poses a particularly high risk for marine organisms inhabiting (sub)-tropical seas, especially for those being restricted to shallow, sunlit waters due to light requirements, such as giant clams and (2) it expands the mutual benefits of the symbiotic relationship between the host and symbiotic unicellular algae, which can be of crucial importance in the oligotrophic water of tropical coral reefs. Further, the photonic cooperation between iridocytes and algal symbionts helps explain the broad color repertoire found for giant clam mantle tissues, ranging from bright blue (corresponding to high iridocyte and low symbiont loads) to dark brown (when the iridocyte load is relatively lower than the number of algal symbionts). Additionally, while giant clams have thus far been used by humans for food and ornamental purposes only, the unique optical properties of their iridocytes, as well as the photonic interaction with the photosynthetic symbionts, may offer a source of bio-inspiration for applications in photonics and other relevant fields.

DATA AVAILABILITY STATEMENT

The datasets generated for this study are available on request to the corresponding author.

AUTHOR CONTRIBUTIONS

SR collected and dissected the animals. RS conducted the experimental measurements. All authors conceived the research, discussed and analyzed the results, and contributed in writing the manuscript.

FUNDING

This research was funded by King Abdullah University of Science and Technology (KAUST) baseline funding to CD. (BAS/1/1071-01-01) and BO (BAS/1/1614-01-01).

ACKNOWLEDGMENTS

We thank Prof. Zhiping Lai for his help with experimental materials and the "Imaging and Characterization Core Lab" of KAUST for support with the SEM and TEM imaging.

SUPPLEMENTARY MATERIAL

The Supplementary Material for this article can be found online at: https://www.frontiersin.org/articles/10.3389/fmars.2020.00465/full#supplementary-material

REFERENCES

Agustí, S., Regaudie-de-Gioux, A., Arrieta, J. M., and Duarte, C. M. (2014). Consequences of UV-enhanced community respiration for plankton metabolic balance. *Limnol. Oceanogr.* 59, 223–232. doi: 10.4319/lo.2014.59.1.0223

Al-Aidaroos, A. M., El-Sherbiny, M. M., Satheesh, S., Mantha, G., Agustî, S., Carreja, B., et al. (2014). High mortality of Red Sea zooplankton under ambient solar radiation. *PLoS One* 9:e108778. doi: 10.1371/journal.pone.0108778

Alcazar, S. N. (1986). Observations on predators of giant clams (Bivalvia: Family *Tridacnidae*). *Silliman J.* 33, 54–57.

Andréfouët, S., Gilbert, A., Yan, L., Remoissenet, G., Payri, C., and Chancerelle, Y. (2005). The remarkable population size of the endangered clam Tridacna maxima assessed in Fangatau Atoll (Eastern Tuamotu. French Polynesia) using in situ and remote sensing data. *ICES J. Mar. Sci.* 62, 1037–1048. doi: 10.1016/j.icesjms.2005.04.006

Aranda, M., Banaszak, A. T., Bayer, T., Luyten, J. R., Medina, M., and Voolstra, C. R. (2011). Differential sensitivity of coral larvae to natural levels of ultraviolet

radiation during the onset of larval competence. *Mol. Ecol.* 20, 2955–2972. doi: 10.1111/j.1365-294x.2011.05153.x

Banaszak, A. T., LaJeunesse, T. C., and Trench, R. K. (2000). The synthesis of mycosporine-like amino acids (MAAs) by cultured, symbiotic dinoflagellates. *J. Exp. Mar. Biol. Ecol.* 249, 219–233. doi: 10.1016/s0022-0981(00)00192-1

Banaszak, A. T., Santos, M. G. B., LaJeunesse, T. C., and Lesser, M. P. (2006). The distribution of mycosporine-like amino acids (MAAs) and the phylogenetic identity of symbiotic dinoflagellates in cnidarian hosts from the Mexican Caribbean. *J. Exp. Mar. Biol. Ecol.* 337, 131–146. doi: 10.1016/j.jembe.2006.06.014

Beckvar, N. (1981). Cultivation, spawning, and growth of the giant clams *Tridacna gigas*, *T. derasa*, and *T. squamosa* in Palau, Caroline Islands. *Aquaculture* 24, 21–30. doi: 10.1016/0044-8486(81)90040-5

Béland, F., Browman, H. I., Rodriguez, C. A., and St-Pierre, J.-F. (1999). Effect of solar ultraviolet radiation (280–400 nm) on the eggs and larvae of Atlantic cod (*Gadus morhua*). *Can. J. Fish. Aquat. Sci.* 56, 1058–1067. doi: 10.1139/f99-039

Bonham, K. (1965). Growth rate of giant clam *Tridacna gigas* at Bikini Atoll as revealed by radioautography. *Science* 149, 300–302. doi: 10.1126/science.149.3681.300

Carreja, B., Fernández, M., and Agustí, S. (2016). Joint additive effects of temperature and UVB radiation on zoeae of the crab *Taliepus dentatus*. *Mar. Ecol. Prog. Ser.* 550, 135–145. doi: 10.3354/meps11715

Chae, J., and Nishida, S. (1994). Integumental ultrastructure and color patterns in the iridescent copepods of the family Sapphirinidae (*Copepoda*: *Poecilostomatoida*). *Mar. Biol.* 119, 205–210. doi: 10.1007/bf00349558

Chew, S. F., Koh, C. Z., Hiong, K. C., Choo, C. Y., Wong, W. P., Neo, M. L., et al. (2019). Light-enhanced expression of Carbonic Anhydrase 4-like supports shell formation in the fluted giant clam *Tridacna squamosa*. *Gene* 683, 101–112. doi: 10.1016/j.gene.2018.10.023

Cloney, R. A., and Brocco, S. L. (1983). Chromatophore organs, reflector cells, iridocytes and leucophores in cephalopods. *Am. Zool.* 23, 581–592. doi: 10.1093/icb/23.3.581

Cohen, I., Dubinsky, Z., and Erez, J. (2016). Light enhanced calcification in hermatypic corals: new insights from light spectral responses. *Front. Mar. Sci.* 2:122. doi: 10.3389/fmars.2015.00122

De Grave, S. (1999). Pontoniinae (*Crustacea*: *Decapoda*: *Palaemonidea*) associated with bivalve molluscs from Hansa Bay, Papua New Guinea. *Bull. Koninklijk Belgisch Inst. Natuurwetensch. Biol.* 69, 125–141.

DeBoer, T. S., Baker, A. C., Erdmann, M. V., Jones, P. R., and Barber, P. H. (2012). Patterns of *Symbiodinium* distribution in three giant clam species across the biodiverse Bird's Head region of Indonesia. *Mar. Ecol. Prog. Ser.* 444, 117–132. doi: 10.3354/meps09413

Deerinck, T. J., Bushong, E. A., Thor, A., and Ellisman, M. H. (2010). *NCMIR Methods for 3D EM: A New Protocol for Preparation of Biological Specimens for Serial Blockface Scanning Electron Microscopy*. Available online at: https://ncmir.ucsd.edu/sbem-protocol/ (accessed June, 2020).

DeMartini, D. G., Ghoshal, A., Pandolfi, E., Weaver, A. T., Baum, M., and Morse, D. E. (2013a). Dynamic biophotonics: female squid exhibit sexually dimorphic tunable leucophores and iridocytes. *J. Exp. Biol.* 216, 3733–3741. doi: 10.1242/jeb.090415

DeMartini, D. G., Krogstad, D. V., and Morse, D. E. (2013b). Membrane invaginations facilitate reversible water flux driving tunable iridescence in a dynamic biophotonic system. *Proc. Natl. Acad. Sci. U.S.A.* 110, 2552–2556. doi: 10.1073/pnas.1217260110

Eliason, C. M., Maia, R., and Shawkey, M. D. (2015). Modular color evolution facilitated by a complex nanostructure in birds. *Evolution* 69, 357–367. doi: 10.1111/evo.12575

Fitt, W. K. (ed.). (1993). "The biology and mariculture of giant clams: a workshop" in *Conjunction with the 7th International Coral Reef Symposiwn 1992* (Guam, USA), ACIAR Proceedings No. 47, 154.

Fox, D. L. (1976). *Animal Biochromes and Structural Colours: Physical, Chemical, Distributional & Physiological Features of Coloured Bodies in the Animal World*. Berkeley, CA: Univ of California Press.

Gao, K., and Zheng, Y. (2010). Combined effects of ocean acidification and solar UV radiation on photosynthesis, growth, pigmentation and calcification of the coralline alga *Corallina sessilis* (*Rhodophyta*). *Global Change Biol.* 16, 2388–2398. doi: 10.1111/j.1365-2486.2009.02113.x

Ghoshal, A., Eck, E., Gordon, M., and Morse, D. E. (2016a). Wavelength-specific forward scattering of light by Bragg-reflective iridocytes in giant clams. *J. R. Soc. Interface* 13:20160285. doi: 10.1098/rsif.2016.0285

Ghoshal, A., Eck, E., and Morse, D. E. (2016b). Biological analogs of RGB pixelation yield white coloration in giant clams. *Optica* 3, 108–111.

Gkikas, D., Argiropoulos, A., and Rhizopoulou, S. (2015). Epidermal focusing of light and modelling of reflectance in floral-petals with conically shaped epidermal cells. *Flora Morphol. Distrib. Funct. Ecol. Plants* 212, 38–45. doi: 10.1016/j.flora.2015.02.005

Gleason, D., and Wellington, G. (1995). Variation in UVB sensitivity of planula larvae of the coral *Agaricia agaricites* along a depth gradient. *Mar. Biol.* 123, 693–703. doi: 10.1007/bf00349112

Glynn, P. (1993). Coral reef bleaching: ecological perspectives. *Coral Reefs* 12, 1–17. doi: 10.1007/bf00303779

Goessling, J. W., Su, Y., Cartaxana, P., Maibohm, C., Rickelt, L. F., Trampe, E. C., et al. (2018). Structure-based optics of centric diatom frustules: modulation of the in vivo light field for efficient diatom photosynthesis. *New Phytol.* 219, 122–134. doi: 10.1111/nph.15149

Goessling, J. W., Wardley, W. P., and Lopez-Garcia, M. (2019). Natural slab photonic crystals in centric diatoms. *bioRxiv* [Preprint]. doi: 10.1101/838185

Gordon, H. R., and Du, T. (2001). Light scattering by nonspherical particles: application to coccoliths detached from *Emiliania huxleyi*. *Limnol. Oceanogr.* 46, 1438–1454. doi: 10.4319/lo.2001.46.6.1438

Griffiths, D., Winsor, H., and Luongvan, T. (1992). Iridophores in the mantle of giant clams. *Austr. J. Zool.* 40, 319–326.

Häder, D.-P., Kumar, H., Smith, R., and Worrest, R. (2007). Effects of solar UV radiation on aquatic ecosystems and interactions with climate change. *Photochem. Photobiol. Sci.* 6, 267–285. doi: 10.1039/b700020k

Häder, D.-P., Williamson, C. E., Wängberg, S. -Å, Rautio, M., Rose, K. C., Gao, K., et al. (2015). Effects of UV radiation on aquatic ecosystems and interactions with other environmental factors. *Photochem. Photobiol. Sci.* 14, 108–126. doi: 10.1039/c4pp90035a

Holm-Hansen, O., and Riemann, B. (1978). Chlorophyll a determination: improvements in methodology. *Oikos* 30, 438–447.

Holt, A. L., Vahidinia, S., Gagnon, Y. L., Morse, D. E., and Sweeney, A. M. (2014). Photosymbiotic giant clams are transformers of solar flux. *J. R. Soc. Interface* 11:20140678. doi: 10.1098/rsif.2014.0678

Ide, H., and Hama, T. (1972). Guanine formation in isolated iridophores from bullfrog tadpoles. *Biochim. Biophys. Gen. Subjects* 286, 269–271. doi: 10.1016/0304-4165(72)90264-4

Ikeda, T., and Kohshima, S. (2009). Why is the neon tetra so bright? Coloration for mirror-image projection to confuse predators¿'Mirror-image decoy" hypothesis. *Environ. Biol. Fishes* 86, 427–441. doi: 10.1007/s10641-009-9543-y

Ip, Y. K., Hiong, K. C., Lim, L. J., Choo, C. Y., Boo, M. V., Wong, W. P., et al. (2018). Molecular characterization, light-dependent expression, and cellular localization of a host vacuolar-type H+-ATPase (VHA) subunit A in the giant clam, *Tridacna squamosa*, indicate the involvement of the host VHA in the uptake of inorganic carbon and its supply to the symbiotic zooxanthellae. *Gene* 659, 137–148. doi: 10.1016/j.gene.2018.03.054

Ip, Y. K., Koh, C. Z., Hiong, K. C., Choo, C. Y., Boo, M. V., Wong, W. P., et al. (2017). Carbonic anhydrase 2-like in the giant clam, *Tridacna squamosa*: characterization, localization, response to light, and possible role in the transport of inorganic carbon from the host to its symbionts. *Physiol. Rep.* 5:e13494. doi: 10.14814/phy2.13494

Ishikura, M., Kato, C., and Maruyama, T. (1997). UV-absorbing substances in zooxanthellate and azooxanthellate clams. *Mar. Biol.* 128, 649–655. doi: 10.1007/s002270050131

Jacobs, M., Lopez-Garcia, M., Phrathep, O.-P., Lawson, T., Oulton, R., and Whitney, H. M. (2016). Photonic multilayer structure of Begonia chloroplasts enhances photosynthetic efficiency. *Nat. Plants* 2:16162.

Jantzen, C., Wild, C., El-Zibdah, M., Roa-Quiaoit, H. A., Haacke, C., and Richter, C. (2008). Photosynthetic performance of giant clams, *Tridacna maxima* and *T. squamosa*, Red Sea. *Mar. Biol.* 155, 211–221. doi: 10.1007/s00227-008-1019-7

Kamishima, Y. (1990). Organization and development of reflecting platelets in iridophores of the giant clam, *Tridacna crocea* Lamarck. *Zool. Sci.* 7, 63–72.

Kanazawa, A., Blanchard, G. J., Szabó, M., Ralph, P. J., and Kramer, D. M. (2014). The site of regulation of light capture in symbiodinium: does the peridinin–chlorophyll a–protein detach to regulate light capture? *Biochim. Biophys. Acta Bioenerget.* 1837, 1227–1234. doi: 10.1016/j.bbabio.2014.03.019

Kawanishi, S., Hiraku, Y., and Oikawa, S. (2001). Mechanism of guanine-specific DNA damage by oxidative stress and its role in carcinogenesis and aging. *Mutat. Res. Rev. Mutat. Res.* 488, 65–76. doi: 10.1016/s1383-5742(00)00059-4

Kim, H. N., Vahidinia, S., Holt, A. L., Sweeney, A. M., and Yang, S. (2017). Geometric design of scalable forward scatterers for optimally efficient solar transformers. *Adv. Mater.* 29:1702922. doi: 10.1002/adma.201702922

Klumpp, D., Bayne, B., and Hawkins, A. (1992). Nutrition of the giant clam *Tridacna gigas* (L.) I. Contribution of filter feeding and photosynthates to respiration and growth. *J. Exp. Mar. Biol. Ecol.* 155, 105–122. doi: 10.1016/0022-0981(92)90030-e

Klumpp, D., and Griffiths, C. (1994). Contributions of phototrophic and heterotrophic nutrition to the metabolic and growth requirements of four species of giant clam (*Tridacnidae*). *Mar. Ecol. Prog. Ser.* 115, 103–115. doi: 10.3354/meps115103

Kobelt, F., and Linsenmair, K. (1992). Adaptations of the reed frog *Hyperolius viridiflavus* (*Amphibia*: *Anura*: *Hyperoliidae*) to its arid environment. *J. Comparat. Physiol. B* 162, 314–326.

LaJeunesse, T. C., Parkinson, J. E., Gabrielson, P. W., Jeong, H. J., Reimer, J. D., Voolstra, C. R., et al. (2018). Systematic revision of symbiodiniaceae highlights the antiquity and diversity of coral endosymbionts. *Curr. Biol.* 28, 2570–2580.

Larkum, T. (1996). How dinoflagellates make light work with peridinin. *Trends Plant Sci.* 1:252. doi: 10.1016/1360-1385(96)81769-9

Leggat, W., Buck, B. H., Grice, A., and Yellowlees, D. (2003). The impact of bleaching on the metabolic contribution of dinoflagellate symbionts to their giant clam host. *Plant Cell Environ.* 26, 1951–1961. doi: 10.1046/j.0016-8025.2003.01111.x

Lesser, M., and Shick, J. (1989). Effects of irradiance and ultraviolet radiation on photoadaptation in the zooxanthellae of *Aiptasia pallida*: primary production, photoinhibition, and enzymic defenses against oxygen toxicity. *Mar. Biol.* 102, 243–255. doi: 10.1007/bf00428286

Lesser, M. P. (1996). Elevated temperatures and ultraviolet radiation cause oxidative stress and inhibit photosynthesis in symbiotic dinoflagellates. *Limnol. Oceanogr.* 41, 271–283. doi: 10.4319/lo.1996.41.2.0271

Lesser, M. P. (2006). Oxidative stress in marine environments: biochemistry and physiological ecology. *Annu. Rev. Physiol.* 68, 253–278. doi: 10.1146/annurev.physiol.68.040104.110001

Llabrés, M., Agustí, S., Fernández, M., Canepa, A., Maurin, F., Vidal, F., et al. (2013). Impact of elevated UVB radiation on marine biota: a meta-analysis. *Global Ecol. Biogeogr.* 22, 131–144. doi: 10.1111/j.1466-8238.2012.00784.x

Locket, N. (1970). Deep-sea fish retinas. *Br. Med. Bull.* 26, 107–111. doi: 10.1093/oxfordjournals.bmb.a070759

Lythgoe, J., Shand, J., and Foster, R. (1984). Visual pigment in fish iridocytes. *Nature* 308, 83–84. doi: 10.1038/308083a0

Maboloc, E. A., Puzon, J. J. M., and Villanueva, R. D. (2015). Stress responses of zooxanthellae in juvenile *Tridacna gigas* (*Bivalvia*, *Cardiidae*) exposed to reduced salinity. *Hydrobiologia* 762, 103–112. doi: 10.1007/s10750-015-2341-y

Mäthger, L. M., and Hanlon, R. T. (2007). Malleable skin coloration in cephalopods: selective reflectance, transmission and absorbance of light by chromatophores and iridophores. *Cell Tissue Res.* 329, 179–186. doi: 10.1007/s00441-007-0384-8

McConnaughey, T., and Whelan, J. (1997). Calcification generates protons for nutrient and bicarbonate uptake. *Earth Sci. Rev.* 42, 95–117. doi: 10.1016/s0012-8252(96)00036-0

Mies, M. (2019). Evolution, diversity, distribution and the endangered future of the giant clam–Symbiodiniaceae association. *Coral Reefs* 38, 1067–1084. doi: 10.1007/s00338-019-01857-x

Mies, M., Dor, P., Güth, A. Z., and Sumida, P. Y. G. (2017). Production in giant clam aquaculture: trends and challenges. *Rev. Fish. Sci. Aquacult.* 25, 286–296. doi: 10.1080/23308249.2017.1285864

Morrison, R. L., Sherbrooke, W. C., and Frost-Mason, S. K. (1996). Temperature-sensitive, physiologically active iridophores in the lizard Urosaurus ornatus: an ultrastructural analysis of color change. *Copeia* 1996, 804–812.

Neo, M. L., Eckman, W., Vicentuan, K., Teo, S. L.-M., and Todd, P. A. (2015). The ecological significance of giant clams in coral reef ecosystems. *Biol. Conserv.* 181, 111–123. doi: 10.1016/j.biocon.2014.11.004

Neo, M. L., and Todd, P. A. (2013). Conservation status reassessment of giant clams (*Mollusca*: *Bivalvia*: *Tridacninae*) in Singapore. *Nat. Singapore* 6, 125–133.

Norton, J., Prior, H., Baillie, B., and Yellowlees, D. (1995). Atrophy of the zooxanthellal tubular system in bleached giant clams *Tridacna gigas*. *J. Invertebr. Pathol.* 66, 307–310. doi: 10.1006/jipa.1995.1106

Norton, J. H., Shepherd, M. A., Long, H. M., and Fitt, W. K. (1992). The zooxanthellal tubular system in the giant clam. *Biol. Bull.* 183, 503–506. doi: 10.2307/1542028

Núñez-Pons, L., Avila, C., Romano, G., Verde, C., and Giordano, D. (2018). UV-protective compounds in marine organisms from the southern ocean. *Mar. Drugs* 16:336. doi: 10.3390/md16090336

Overmans, S., and Agustí, S. (2019). Latitudinal gradient of UV attenuation along the highly transparent red sea basin. *Photochem. Photobiol.* 95, 1267–1279. doi: 10.1111/php.13112

Overmans, S., and Agustí, S. (2020). Unraveling the seasonality of UV exposure in reef waters of a rapidly warming (sub-) tropical sea. *Front. Mar. Sci.* 7:111. doi: 10.3389/fmars.2020.00111

Pappas, M. K., He, S., Hardenstine, R. S., Kanee, H., and Berumen, M. L. (2017). Genetic diversity of giant clams (*Tridacna* spp.) and their associated Symbiodinium in the central Red Sea. *Mar. Biodivers.* 47, 1209–1222. doi: 10.1007/s12526-017-0715-2

Quintero-Torres, R., Aragón, J., Torres, M., Estrada, M., and Cros, L. (2006). Strong far-field coherent scattering of ultraviolet radiation by holococcolithophores. *Phys. Rev. E* 74:032901.

Ravanat, J.-L., Douki, T., and Cadet, J. (2001). Direct and indirect effects of UV radiation on DNA and its components. *J. Photochem. Photobiol. B Biol.* 63, 88–102. doi: 10.1016/s1011-1344(01)00206-8

Regaudie-de-Gioux, A., Agustí, S., and Duarte, C. M. (2014). UV sensitivity of planktonic net community production in ocean surface waters. *J. Geophys. Res. Biogeosci.* 119, 929–936. doi: 10.1002/2013jg002566

Rohrlich, S. T., and Rubin, R. W. (1975). Biochemical characterization of crystals from the dermal iridophores of a chameleon *Anolis carolinensis*. *J. Cell Biol.* 66, 635–645. doi: 10.1083/jcb.66.3.635

Rosic, N. N., and Dove, S. (2011). Mycosporine-like amino acids from coral dinoflagellates. *Appl. Environ. Microbiol.* 77, 8478–8486. doi: 10.1128/aem.05870-11

Rossbach, S., Saderne, V., Anton, A., and Duarte, C. M. (2019). Light-dependent calcification in red sea giant clam *Tridacna maxima*. *Biogeosciences* 16, 2635–2650. doi: 10.5194/bg-16-2635-2019

Scholander, P. (1954). Secretion of gases against high pressures in the swimbladder of deep sea fishes II. The rete mirabile. *Biol. Bull.* 107, 260–277. doi: 10.2307/1538612

Setoguti, T. (1967). Ultrastructure of guanophores. *J. Ultrastruc. Res.* 18, 324–332. doi: 10.1016/s0022-5320(67)80121-7

Shick, J., Lesser, M., Dunlap, W., Stochaj, W., Chalker, B., and Won, J. W. (1995). Depth-dependent responses to solar ultraviolet radiation and oxidative stress in the zooxanthellate coral *Acropora microphthalma*. *Mar. Biol.* 122, 41–51. doi: 10.1007/bf00349276

Shick, J. M., Dunlap, W. C., Chalker, B. E., Banaszak, A. T., and Rosenzweig, T. K. (1992). Survey of ultraviolet radiation-absorbing mycosporine-like amino acids in organs of coral reef holothuroids. *Mar. Ecol. Prog. Ser.* 90, 139–148. doi: 10.3354/meps090139

Shick, J. M., Lesser, M. P., and Jokiel, P. L. (1996). Effects of ultraviolet radiation on corals and other coral reef organisms. *Global Change Biol.* 2, 527–545. doi: 10.1111/j.1365-2486.1996.tb00065.x

Sinha, R. P., Singh, S. P., and Häder, D.-P. (2007). Database on mycosporines and mycosporine-like amino acids (MAAs) in fungi, cyanobacteria, macroalgae, phytoplankton and animals. *J. Photochem. Photobiol. B Biol.* 89, 29–35. doi: 10.1016/j.jphotobiol.2007.07.006

Smith, R. C., and Baker, K. S. (1979). Penetration of UV-B and biologically effective dose-rates in natural waters. *Photochem. Photobiol.* 29, 311–323. doi: 10.1111/j.1751-1097.1979.tb07054.x

Sun, J., Bhushan, B., and Tong, J. (2013). Structural coloration in nature. *Rsc Adv.* 3, 14862–14889.

Tam, H. L., Cheah, K. W., Goh, D. T., and Goh, J. K. (2013). Iridescence and nanostructure differences in Papilio butterflies. *Opt. Mater. Express* 3, 1087–1092.

Taylor, D. L. (1969). Identity of zooxanthellae isolated from some Pacific *Tridacnidae*. *J. Phycol.* 5, 336–340. doi: 10.1111/j.1529-8817.1969.tb02623.x

Teyssier, J., Saenko, S. V., Van Der Marel, D., and Milinkovitch, M. C. (2015). Photonic crystals cause active colour change in chameleons. *Nat. Commun.* 6:6368.

Théry, M., and Casas, J. (2002). Visual systems: predator and prey views of spider camouflage. *Nature* 415:133. doi: 10.1038/415133a

Trench, R., Wethey, D., and Porter, J. (1981). Observations on the symbiosis with zooxanthellae among the *Tridacnidae* (*Mollusca*, *Bivalvia*). *Biol. Bull.* 161, 180–198. doi: 10.2307/1541117

Van De Poll, W. H., Eggert, A., Buma, A. G., and Breeman, A. M. (2001). Effects of UV-B-induced DNA damage and photoinhibition on growth of temperate marine red macrophytes: habitat-related differences in UV-B tolerance. *J. Phycol.* 37, 30–38. doi: 10.1046/j.1529-8817.2001.037001030.x

Van Wynsberge, S., Andréfouët, S., Gaertner-Mazouni, N., Wabnitz, C. C. C., Gilbert, A., Remoissenet, G., et al. (2016). Drivers of density for the exploited giant clam *Tridacna maxima* : a meta-analysis. *Fish Fish.* 17, 567–584. doi: 10.1111/faf.12127

Vértesy, Z., Bálint, Z., Kertész, K., Vigneron, J., Lousse, V., and Biró, L. (2006). Wing scale microstructures and nanostructures in butterflies- natural photonic crystals. *J. Microsc.* 224, 108–110. doi: 10.1111/j.1365-2818.2006.01678.x

Vicentuan-Cabaitan, K., Neo, M. L., Eckman, W., Teo, S. L., and Todd, P. A. (2014). Giant clam shells host a multitude of epibionts. *Bull. Mar. Sci.* 90, 795–796. doi: 10.5343/bms.2014.1010

Yonge, C. (1975). Giant clams. *Sci. Am.* 232, 96–105. doi: 10.1038/scientific american0475-96

Conflict of Interest: The authors declare that the research was conducted in the absence of any commercial or financial relationships that could be construed as a potential conflict of interest.